Journal of Nuclear Materials 390–391 (2009) 1097–1101

Contents lists available at ScienceDirect

Journal of Nuclear Materials

journal homepage: www.elsevier.com/locate/jnucmat

Temperature measurement of plasma-facing surfaces in tokamaks by active pyrometry

V. Grigorova [a], A. Semerok [a], D. Farcage [a], J.M. Weulersse [a], P.Y. Thro [a,*], E. Gauthier [b], H. Roche [b], Th. Loarer [b], Ch. Grisolia [b]

[a] CEA Saclay, DEN/DPC/SCP/LILM, Bat. 467, 91191 Gif-sur-Yvette, France
[b] CEA Cadarache, DSM/ IRFM/SIPP, 13108 Saint Paul Lez Durance, France

A B S T R A C T

This paper discusses feasibility and tests of a new method for in situ temperature measurement of tokamak plasma-facing metallic surfaces under plasma presence. In such conditions, the other temperature-measurement methods are not applicable due to the perturbing thermal radiation reflected by the walls. Our approach overcomes this limitation by looking with two pyrometers to the measured surface while thermally perturbed. Because of the thermal perturbation each pyrometer records a signal modulation. The temperature, deduced by the ratio between the two signal modulations is dependent neither on the environmental reflecting fluxes nor on the surface emissivity. Originally, the measured temperature is linked to the signals ratio via the experimental set-up parameters. Here, we proposed an alternative way to deduce it from the pyrometers calibration data only. With this method we obtained temperature measurements with accuracy better than 90%.

1. Introduction

Presence of plasma inside tokamak-type reactor defines special requirements concerning the wall materials. At present, the JET (Joint European Torus, Culham, UK) wall tiles are made of beryllium and carbon and in near future will be covered by tungsten. In normal working conditions, their surface temperature varies from about 300 °C up to about 1500 °C and should remain much below the fusion temperature of the material. Nowadays, the widest-used technique for following wall-surface temperatures in this domain is infrared thermography. This technique, however, has two limiting disadvantages: the measurements are perturbed by the surrounding thermal radiations reflected by the observed surface and the temperature values depend on the emissivity of the measured surface. Hence, being able to follow wall-surface temperature under extreme conditions (such as plasma presence) becomes an important issue, especially in the perspective of ITER (International Thermonuclear Experimental Reactor, Cadarache, France). The main drawbacks of infrared thermography are overcome by a new method for remote contactless temperature measurement by optical detection and modulated heating. Unlike the classical pyrometry operating with a single detector, the proposed method registers the temperature by two detectors working at different but close mean wavelengths. The studied surface is subject to small thermal perturbations aimed to modulate its temperature. As a result, each of the optical detectors records a modulated signal. The temperature deduced by the ratio between the two modulated signals is independent of the reflected fluxes as well as of the surface emissivity. Basic theoretical development of that method was done by Berthet et al. [1] and preliminary tests were performed by Loarer et al. [2,3]. The aim of this study was realisation and preliminary testing of a laboratory set-up of the method, which is planned further to be used for in situ measurements at JET. The studied method can be implemented not only in tokamak but also where remote contactless temperature measurements, unperturbed by reflected heat fluxes and by variable emissivity coefficients are needed.

2. Temperature measurement: theoretical background

A radiation flux Φ emitted by a body can be split into two parts: the flux Φ_{emitt} emitted by the body itself due to its temperature and a reflected flux Φ_{refl} due to the environment:

$$\Phi = \Phi_{emitt} + \Phi_{refl} = \varepsilon_\lambda \times L^0_\lambda(T_0) + \Phi_{refl}(T_{surr}), \quad (1)$$

where ε_λ is the emissivity of the treated sample at the working wavelength λ and $L^0_{T,\lambda}$ [W m^{-3} str^{-1}] is the surface spectral radiance at wavelength λ and temperature T.

In order to measure the surface temperature T_0 of that body in such a way that the measured value is not affected by the body emissivity ε and by the surroundings, (i.e. to realise our method),

* Corresponding author.
E-mail address: pierre-yves.thro@cea.fr (P.Y. Thro).

0022-3115/$ - see front matter © 2009 Published by Elsevier B.V.
doi:10.1016/j.jnucmat.2009.01.278

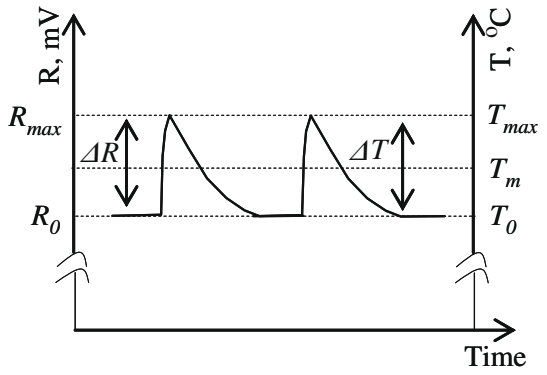

Fig. 1. Signal modulations and temperature ones.

a small thermal perturbation is applied to the studied surface. The perturbation ΔT must be small by comparison to the absolute surface temperature T_0. If the thermal reaction of the body to that perturbation is followed by a filter-equipped optical detector (pyrometer), we can record a signal modulation ΔR (see Fig. 1) related to the detector parameters and to the surface thermal conditions as follows:

$$\begin{aligned}\Delta R = &\underbrace{S \times \Omega}_{\text{Geometrical parameters}} \times \underbrace{r}_{\text{Electrical parameter}} \times \underbrace{D_\lambda \times \tau_\lambda \times \Delta\lambda}_{\text{Optical parameters}} \times \int_{T_0}^{T_0+\Delta T} \\ &\times \frac{\partial}{\partial T_0}(\varepsilon_\lambda \times L^0_\lambda(T_0) + \Phi_{refl}(T_{surr})) \times \mathrm{d}T \\ &= S \times \Omega \times r \times \varepsilon_\lambda \times D_\lambda \times \tau_\lambda \times \Delta\lambda \times \int_{T_0}^{T_0+\Delta T} \frac{\partial L^0_{\lambda,T}}{\partial T} \times \mathrm{d}T,\end{aligned} \tag{2}$$

where: S, m^2 – perturbed zone surface; Ω, str – pyrometer's solid angle; r, $V\,A^{-1}$ – pyrometer's electrical resistance; D_λ, $A\,W^{-1}$ – detector's sensitivity; τ_λ – optical transmissivity at wavelength λ; $\Delta\lambda$, m – pyrometer's spectral bandwidth.

To avoid the influence of the surface emissivity on the measured values, we follow the surface thermal reaction not with one but with two pyrometers, working at different-but-close-one-to-another wavelengths (i.e. $\bar\lambda_1 \neq \bar\lambda_2$ and $\bar\lambda_1/\bar\lambda_2 \to 1$). Like this the surface emissivity for both detectors will be almost the same: $\varepsilon_1 \approx \varepsilon_2$, and hence their ratio will be taken equal to one: $\varepsilon_1/\varepsilon_2 \approx 1$. Therefore, the ratio between the signal modulations of the two detectors will be independent on the surface emissivity.

As both pyrometers take signal from the same perturbed zone $S_1 = S_2 = S$, Eq. (4) may be simplified as follows:

$$\frac{\Delta R_1}{\Delta R_2} \approx \frac{\Omega_1 \times r_1 \times D_{\lambda 1} \times \tau_{\lambda 1} \times \Delta\lambda_1 \times \int_{T_0}^{T_0+\Delta T} \frac{\partial L^0_{\lambda 1}}{\partial T}\mathrm{d}T}{\Omega_2 \times r_2 \times D_{\lambda 2} \times \tau_{\lambda 2} \times \Delta\lambda_2 \times \int_{T_0}^{T_0+\Delta T} \frac{\partial L^0_{\lambda 1}}{\partial T}\mathrm{d}T}. \tag{3}$$

Writing $\Omega_i \times r_i \times D_{\lambda i} \times \tau_{\lambda i} \times \Delta\lambda_i = Z_i$, ($i$ = 1 and 2), Eq. (3) may be given in more compact form:

$$\frac{\Delta R_1}{\Delta R_2} = \frac{Z_1 \times \int_{T_0}^{T_0+\Delta T} \frac{\partial L^0_{\lambda 1}}{\partial T}\mathrm{d}T}{Z_2 \times \int_{T_0}^{T_0+\Delta T} \frac{\partial L^0_{\lambda 2}}{\partial T}\mathrm{d}T}. \tag{4}$$

Via Eq. (4), we can deduce the surface temperature T_0 from the ratio of measured signal modulations of the two pyrometers without being affected by the reflected flux and by the surface emissivity: the right-hand side ratio only depends on T_0 if Z_1 and Z_2 are known, so the measured ratio $\Delta R_1/\Delta R_2$ univocally gives T_0.

Further simplification can be made by assuming that the spectral radiance derivative $\partial L^0_\lambda/\partial T$ is constant over the temperature range ($T_0 + \Delta T$). This is approximately the case if $\partial L^0_\lambda/\partial T$ is computed at ($T_0 + \Delta T$)/2 (see Fig. 2). Eq. (4) becomes then:

$$\frac{\Delta R_1}{\Delta R_2} \approx \frac{Z_1 \times \left(\frac{\partial L^0_{\lambda 1}}{\partial T}\right)_{@(T_0+\Delta T)/2} \times \Delta T}{Z_2 \times \left(\frac{\partial L^0_{\lambda 2}}{\partial T}\right)_{@(T_0+\Delta T)/2} \times \Delta T}. \tag{5}$$

3. Laboratory feasibility of temperature measurement with two pyrometers on CFC sample

The aim of this study is to test the accuracy of the method in perspective of its future application to JET. For this, we compared measurements obtained both by proposed method and by a single IR detector. Classical pyrometry (i.e. single IR detector technique) gives correct responses only at high emissivity surfaces and in absence of reflecting fluxes. This is why, as a first step, the experiments were carried out in these conditions.

3.1. Experimental set-up

The experimental set-up consists of two pyrometers Kleiber 740-LO, two external interferential band pass filters, a Carbon Fibre Composite (CFC) sample and an infrared Nd:YAG laser (see Fig. 3). Pyrometer 1 operates in the temperature range (300–2300 °C) and in the spectral band (2.0–2.2 μm) with a response time of 10 μs. Pyrometer 2 operates between 200 and 1000 °C and in the spectral band (1.58–2.2 μm) with the same response time. Both pyrometers have the same photosensitive element. The external band pass filter coupled with pyrometer 1 has a mean wavelength of 2092 nm, a mean spectral bandwidth of 84 nm and maximal transmissivity of 84%. The external filter coupled with pyrometer 2 has a mean wavelength of 1668.5 nm, a mean spectral band width of 29 nm and a maximal transmissivity of 79%. The CFC sample is 30 mm wide, 30 mm long and 10 mm thick. The pulsed Nd:YAG laser, emitting at 1064 nm, has a maximal average output power of 300 W and a repetition rate varying from 20 Hz up to 10 kHz. For

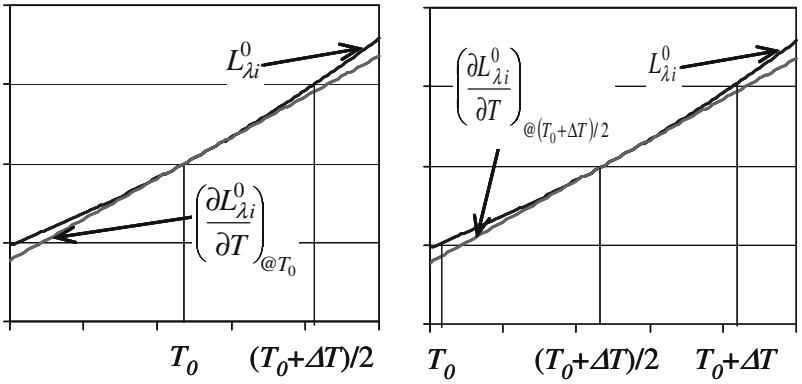

Fig. 2. Spectral radiance curve and spectral radiance derivative one while: (a) calculating the derivative at T_0; (b) calculating the derivative at ($T_0 + \Delta T$)/2.

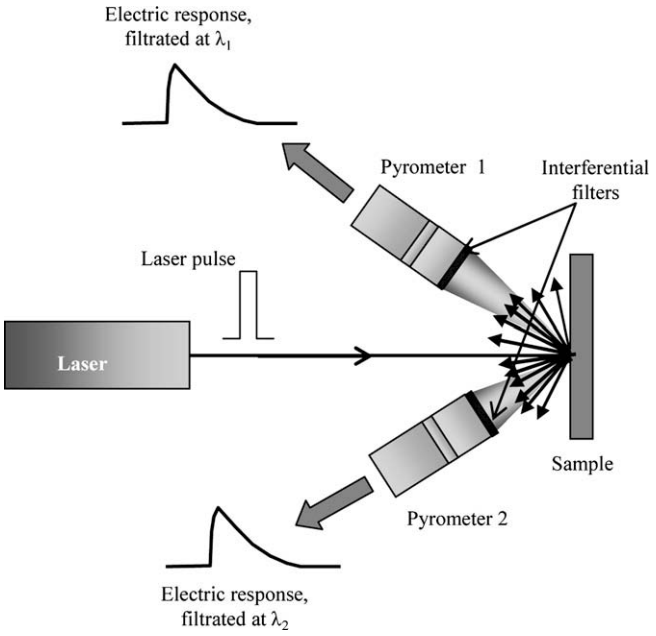

Fig. 3. Scheme of the laser heating experimental set-up.

Table 1
Calibration constants under ambient conditions.

	$k_{i,1}$	$k_{i,2}$	$k_{i,3}$
Pyrometer 1 ($i = 1$)	519.8	−21.60	−70.87
Pyrometer 2 ($i = 2$)	233.1	19.37	156.1

the experiments described here, the repetition rate was set at 500 Hz and the pulse duration was 1 ms.

3.2. Pyrometer calibration

Pyrometer calibrations were done under ambient conditions for a black-body temperature range between 400 and 900 °C. Obtained signal was observed with an oscilloscope. By processing the experimental data we established the $T = f(R)$ function of the calibration equations:

$$T_i = k_{i,1} \times R_i^{0.2} + k_{i,2} \times \ln(R_i) + k_{i,3}. \quad (6)$$

The calibration constants values for each pyrometer are listed in Table 1. Eq. (6) is visualised in Figs. 4 and 5 for pyrometer 1 and pyrometer 2, respectively.

3.3. Remark on sample heating

Before inducing thermal perturbations, the studied sample has to be heated so that its temperature being high enough to be recorded by the pyrometers. Let remind that a reason for heating the sample is also to be representative of the temperature conditions expected on the tokamak wall. Initially, we tried to heat the sample by hot-air blowpipes but the maximal temperature obtained by this way was only 450 °C. For this reason, we decided to use the laser both for heating and inducing thermal perturbation. A scheme of the realised experimental set-up is given in Fig. 3.

4. Results and analyses

We performed series of experiments at four different laser average powers, namely 101, 105, 113 and 165 W. Fig. 6 presents the

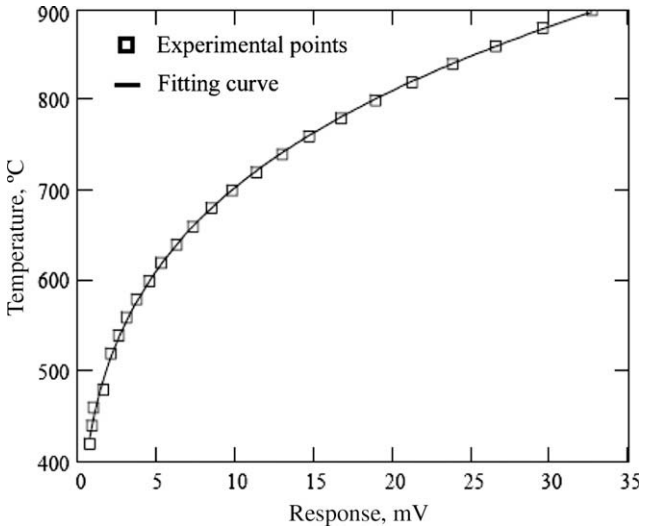

Fig. 4. Calibration curve of pyrometer 1.

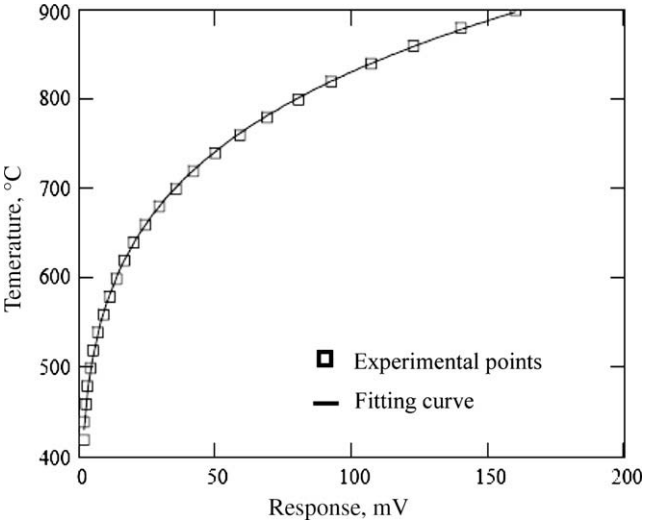

Fig. 5. Calibration curve of pyrometer 2.

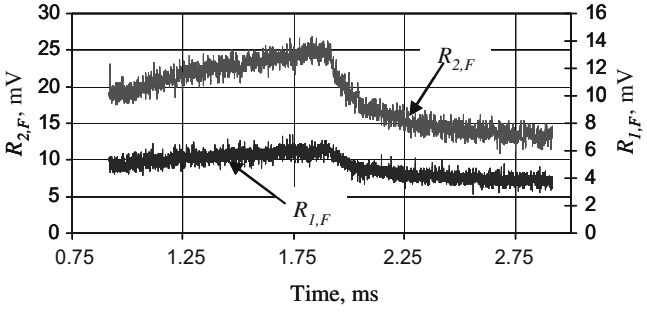

Fig. 6. Pyrometers responses in respect to time.

measured signal modulations of both pyrometers and Fig. 7 visualises the corresponding temperatures for laser mean power of 105 W. Temperature measurement uncertainties in all experiments were less than 1%. The slight difference of about 20 K between the temperature values given by the two detectors (see Fig. 7) is due to the fact that the external filters were heated by the surroundings. We measured that their surface temperatures

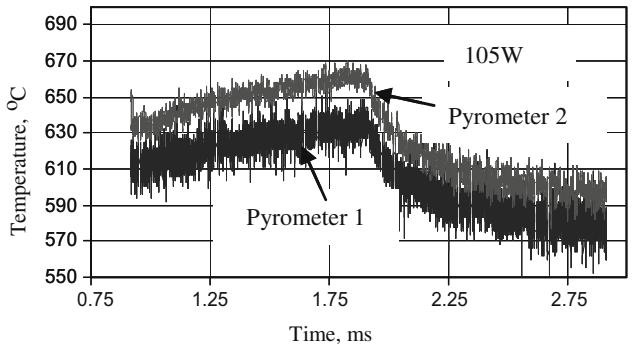

Fig. 7. Temperature of pyrometer 1 and pyrometer 2 at 105 W laser mean power.

Table 2
Calibration constants under ambient conditions.

$R = f(T)$	$j_{i,1}$	$j_{i,2}$	$j_{i,3}$	$j_{i,4}$
Pyrometer 1 ($i = 1$)	-3.117×10^{-8}	0.391	8.394×10^{-11}	4
Pyrometer 2 ($i = 2$)	-5.155×10^{-10}	-1.875×10^{-18}	3.037×10^{-16}	6

were increased up to about 60 °C. Being interferential ones, the filters change slightly their maximal transmissivity and mean wavelength at high temperatures, which, in turn, changes the detectors sensitivity. Besides, the filter of pyrometer 1 is stronger affected by this effect as being closer to the heated sample. Under tokamak conditions, however, such thermal effect on filters would not exist.

The ratio curve should be originally calculated by Eq. (3). But certain characteristics of both detectors are unknown (electrical resistance r and detector sensitivity D_λ). Hence, we cannot calculate the ratio curve using the approach proposed by [1–3]. But the calibration procedure gave us empirical numerical relation between signal and temperature for both pyrometers. Mathematically speaking, the relation between signal modulation and temperature is the derivative in respect to temperature of the calibration equations in their $R = f(T)$ mode:

$$\Delta R = Z \times \left(\frac{\partial L_T^0}{\partial T}\right) \mathrm{d}T = \frac{\partial R}{\partial T}. \tag{7}$$

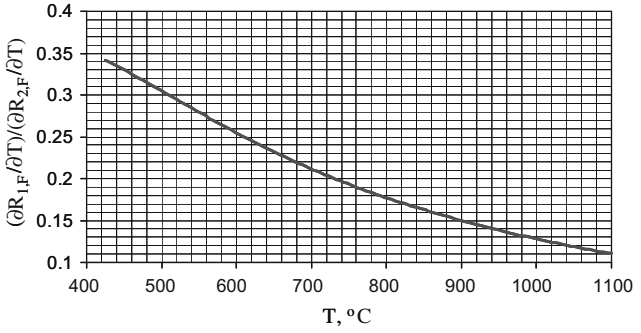

Fig. 8. Ratio curve.

Hence, the ratio curve may be computed as follows:

$$\frac{\Delta R_1}{\Delta R_2} = \frac{\partial R_1/\partial T}{\partial R_2/\partial T}. \tag{8}$$

The $R = f(T)$ general mode of the calibration equations (again R in mV and T in °C) is given by Eq. (9). Eq. (10) relates signal modulation (in mV K^{-1}) to temperature (in °C):

$$R_i = j_{i,1} T_i^3 + j_{i,2} \ \exp(T_i^{-1}) + j_{i,3} T_i^{j_4} \tag{9}$$

$$\frac{\partial R_i}{\partial T} = 3j_{i,1} \times T_i^2 - j_{i,2} \times T_i^{-2} \times \exp(T_i^{-1}) + j_{i,3} \times j_{i,4} \times T_i^{(j_{i,4}-1)}. \tag{10}$$

The fitting is performed by the method of least squares. The calibration constants for both detectors are listed in Table 2.

Substituting Eq. (10) in Eq. (8) gives the final mode of the ratio curve equation:

$$\frac{\Delta R_1}{\Delta R_2} = \frac{3j_{1,1} \times T^2 - j_{1,2} \times T^{-2} \times \exp(T^{-1}) + j'_{1,3} \times j_{1,4} \times T^{(j_{1,4}-1)}}{3j_{2,1} \times T^2 - j_{2,2} \times T^{-2} \times \exp(T^{-1}) + j'_{2,3} \times j_{2,4} \times T^{(j_{2,4}-1)}}. \tag{11}$$

Fig. 8 visualises the ratio curve we got from Eq. (11). To the aim of testing its accuracy, we compared the experimentally measured mean temperature $T_{experiment}$ to the temperature, deduced by the ratio curve T_{model} (Fig. 8). The experimentally measured surface temperature $T_{0,experiment}$ is computed as follows:

$$T_{0,experiment} = \frac{T_{0,1} + T_{0,2}}{2}. \tag{12}$$

The model prediction error is estimated by the following formula:

$$Error = \frac{\bar{T}_{model} - \bar{T}_{experiment}}{\bar{T}_{model}} \times 100\%. \tag{13}$$

For 105 W laser mean power (see Fig. 7) the surface temperature measured by pyrometer 1 and by pyrometer 2 is $T_{0,1}$ = 580 °C and $T_{0,2}$ = 600 °C, respectively. The mean experimental temperature is calculated by Eq. (12): $T_{0,experiment}$ = 590 °C = 863 K. Fig. 6 reports signal modulation of pyrometer 1 and of pyrometer

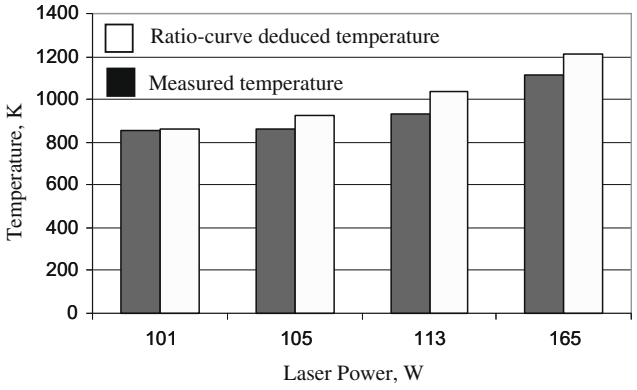

Fig. 9. Ratio curve prediction precision.

Table 3
Model prediction error.

Laser mean power	$T_{0,1}$	$T_{0,2}$	$T_{0,experiment}$		ΔR_1	ΔR_2	Ratio	$T_{0,model}$		Error
W	°C	°C	°C	K	mV	mV	–	°C	K	%
101	580	580	580	853	2.1	8	0.26	590	863	1.2
105	580	600	590	863	2.5	11	0.23	650	923	6.5
113	650	670	660	933	5	27	0.19	760	1033	9.7
165	830	850	840	1113	10	70	0.14	940	1213	8.2

2, 2.5 and 11 mV, respectively. Hence, the signal modulation ratio is 2.5/11 = 0.23. According to Fig. 8, a ratio of 0.23 corresponds to a model surface temperature of 650 °C, i.e., $T_{0,model}$ = 650 °C = 923 K. Hence, the prediction error calculated by Eq. (13) is 6.5%. The results for all four examined laser mean powers, namely 101, 105, 113 and 165 W, are presented in Table 3 and in Fig. 9.

5. Conclusions

We reported here first experimental tests of a method dedicated to the measurement of surface temperature under tokamak conditions. In principle, this method is able to retrieve the temperature despite an unknown surface emissivity and perturbing reflected fluxes. As a first step we compared the proposed method with classical pyrometry and found accuracy better than 90%. These encouraging results will be followed in the near future by experiment in more real conditions where the main advantages of the method could be demonstrated in practice.

Acknowledgement

This work was performed within the frames of the EFDA JET Fusion Technology Programme, Task JW6-FT-3.37.

References

[1] O. Berthet et al, Process for Measuring the Temperature of a Body by Optical Detection and Modulated Heating, United States Patent 4799788, 24 January 1989.
[2] Th. Loarer, Mesure de Température de Surface par Effet Photothermique modelé ou Impulsionnel, PhD Dissertation, Laboratoire E.M2.C, UPR 288 CNRS and Ecole Centrale Paris, 1989.
[3] Th. Loarer et al., JNM 363–365 (2007) 1450.